Graphene Platform for Hairpin-DNA-Based Impedimetric Genosensing

Alessandra Bonanni and Martin Pumera*

Division of Chemistry & Biological Chemistry, School of Physical and Mathematical Sciences, Nanyang Technological University, Singapore 637371

ABSTRACT There is enormous need for sensitive and selective detection of single nucleotide polymorphism of a DNA strand as this issue is related to many major diseases and disorders, such as Parkinson's and Alzheimer's disease. To achieve sensitivity and selectivity of the detection, a highly sensitive transducer of the signal with high surface area is required. In this work we employ a graphene platform to combine the sensitivity of electrochemical impedance spectroscopy with the high selectivity of hairpin-shaped DNA probes for the rapid detection of single nucleotide polymorphism correlated to the development of Alzheimer's disease. We investigate the influence of various graphene platforms consisting of different numbers of same-sized graphene layers. We believe that our findings are an important step toward highly sensitive and selective sensing architectures.

KEYWORDS: graphene · impedance spectroscopy · hairpin-DNA · genosensor · single nucleotide polymorphism

There is enormous demand for new tools in biomedical point-of-care detection due to the aging population in the first world countries. The need for rapid and sensitive DNA analysis is becoming a very important issue in clinical diagnosis. DNA biosensor technologies are rapidly developing as a valid alternative to classical gene assay,[1−5] not only for the well-known advantages they provide such as low cost, simplicity, and possibility of miniaturization[6,7] but also for their application in the rapid and sensitive detection of single nucleotide polymorphisms.[8−11] A single nucleotide polymorphism (SNP) is a DNA sequence variation occurring when a single nucleotide in the genome differs between members of the same species.[12,13] SNPs can occur in every 100−300 base pairs and have been correlated to the development of different diseases and genetic disorders such as cystic fibrosis, Alzheimer's disease, Parkinson's disease, diabetes, and various cancers.[14] The early identification of SNPs provides an opportunity for rapid diagnosis and treatment of disease.

A major concern in biosensing is the low capabilities shown by existing platforms to selectively discriminate a complementary sequence from one containing SNPs. To overcome this problem we immobilized hairpin-DNA (hpDNA) probes onto the electrode surface. HpDNA is a secondary DNA structure in which two regions of the same strand, complementary in nucleotide sequence, base-pair between each other to form a double helix that ends in an unpaired loop.[15,16] Owing to its inherent structural constraint, hpDNA presents a higher selectivity for target recognition capabilities in the presence of SNPs when compared with linear DNA probes.[17−20] The combination of graphene oxide (GO) and hpDNA was recently used by a few groups for the detection of SNPs in solution using fluorescence assay.[21,22] However, for the development of user-friendly and nonexpensive portable devices for point-of-care diagnostic tests, electrochemistry-based detection would be the best choice, given its inherent miniaturization capability and compatibility with advanced microfabrication schemes.[23−25]

In this work we employ and compare for the first time different graphene platforms modified with hpDNA probes for the sensitive detection of SNP correlated to the development of Alzheimer's disease, using graphene as transducer and electrochemical impedance spectroscopy (EIS) as a highly sensitive detection technique. Graphene-based nanomaterials exhibit advantages over other electrode materials in terms of high 2-D electrical conductivity, very fast heterogeneous electron transfer, and high surface area.[26−28] EIS is a characterization technique that provides electrical information in the frequency domain.[29,30] Because of its ability for probing the interfacial properties at the electrode surface and the possibility of performing label-free detections, EIS is increasingly being used for the very sensitive detection of biorecognition events at the electrode surface.[31,32] Here we compare graphene nanomaterials with a different number of stacked sheets,

* Address correspondence to pumera@ntu.edu.sg.

Received for review January 10, 2011 and accepted February 16, 2011.

Published online February 28, 2011
10.1021/nn200091p

© 2011 American Chemical Society

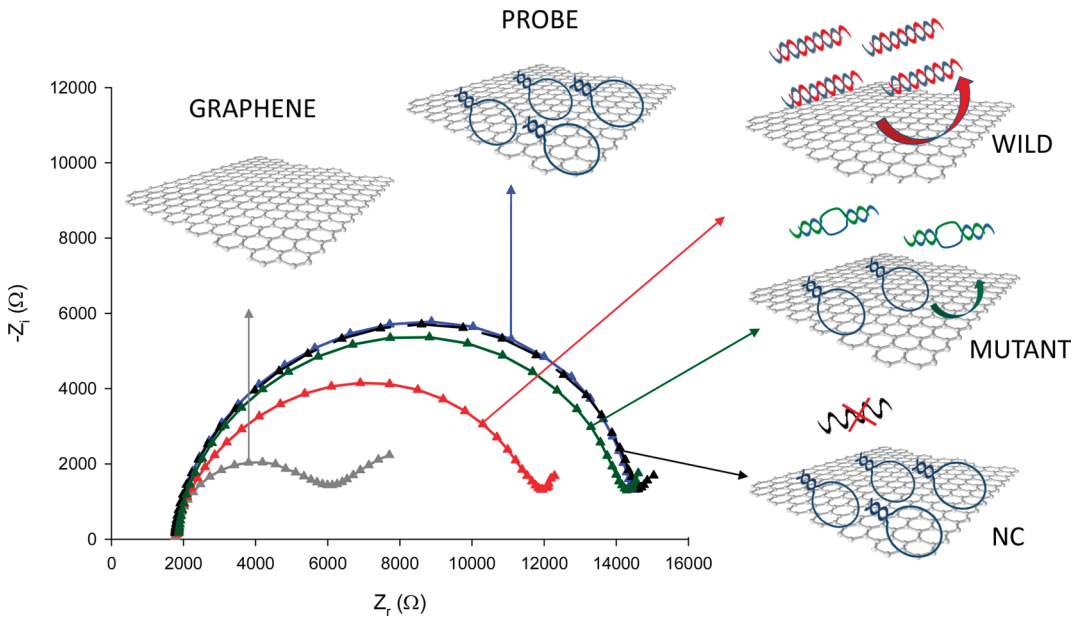

Figure 1. Schematic of the protocol and Nyquist plots, $-Z_i$ *vs* Z_r, of the graphene surface (gray), hpDNA (blue), complementary target (red), 1-mismatch target (green), and negative control with a noncomplementary sequence (black) (concentration of the DNA probes, 1×10^{-5} M; concentration of the DNA target, 3×10^{-8} M). All measurements were performed in 0.1 M PBS buffer solution containing 10 mM $K_3[Fe(CN)_6]/K_4[Fe(CN)_6]$.

and we find out that, interestingly, the single sheet graphene does not provide the highest reliability. Our investigation shall have profound impact on the design of graphene-based DNA sensors.

RESULTS AND DISCUSSION

We investigated in this work the suitability of different graphene surfaces for hairpin impedimetric genosensing. We employed graphene nanoribbons consisting mostly of single- and double-layered graphene (marked as G-SL) (note that in electrochemistry the bulk amount of materials are usually needed and pure single or double sheet graphenes are not available in bulk quantities); triple and four layer graphenes (G-FL), and multilayer graphene nanoribbons (G-ML). All graphene materials had a base size of graphene sheet about 100×100 nm^2. For detailed characterization see Supporting Information.

HpDNA probes were immobilized on the graphene-modified electrode surface by physical adsorption. The π-stacking interactions between the ring of nucleobases and the hexagonal cells of graphene make the platform a stable substrate for genosensing. As reported in previous work, partial release of the hpDNA probes from the graphene surface occurs as a consequence of hybridization with complementary target. In fact, the formation of stable hydrogen bonds among nucleobases and their shielding inside the phosphate backbone after hybridization is the driving force for the above-mentioned release. Different DNA sequences correlated to Alzheimer's disease were used in this work. Alzheimer's disease (AD) is a neurodegenerative disorder which affects millions of people in the aging population worldwide.[33] One genetic risk factor for the development of the disease is the presence of a mutation in the Apolipoprotein E (apo-E) gene.[34] The apo-E gene is polymorphic and presents a dysfunctional allele (apo-E4) in which a thymine is replaced by a cytosine.[35] The presence of this mutation is involved in the development of the disorder. The complementary target (wild-type) used in our experiments corresponds to the nonmutated Apo-E gene. The target with one mutation (mutant) corresponds to the dysfunctional allele (apo-E4).[36] The noncomplementary target (nc) was used for control experiments.

Figure 1 shows the Nyquist plots obtained in a whole impedimetric experiment and a general scheme of the graphene-based sensing platform. A Randles equivalent circuit $R_1(Q[R_2W])$ was used to fit the experimental data (for more details refer to Supporting Information). Among the electrical parameters, we focused on the change of the charge transfer resistance (R_{ct}) value (R_2 in the circuit) recorded after any further step in the biosensing protocol. In fact, the charge transfer process, due to the redox reaction of the couple $K_3[Fe(CN)_6]/K_4[Fe(CN)_6]$ at the applied potential, is strongly influenced by any electrode surface modification. In the Nyquist plot, the R_{ct} value corresponds to the diameter of the semicircle. Figure 1 shows that the R_{ct} of the graphene-modified electrode (gray color) significantly increased after hpDNA probes immobilization (blue color) onto the sensor surface. This is due to hindrance of the electron transfer process of $[Fe(CN)_6]^{3-/4-}$ at the electrode surface after modification.[31] The negative charges on the phosphate backbone of the immobilized hpDNA probes repelled

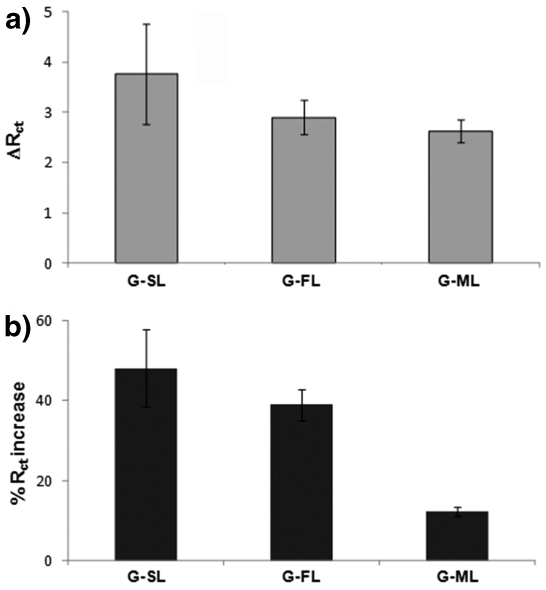

Figure 2. Histogram representing a comparison of impedimetric signal on G-SL, G-FL, and G-ML after (a) hpDNA immobilization; signal is represented as $\Delta R_{ct} = R_{ct(probe)}/R_{ct(blank)}$; (b) hybridization with the complementary target (wild-type). Signal is represented as % R_{ct} increase = $(\Delta_{ratio(nc)}/\Delta_{ratio(wild)} - 1) \times 100$. Error bars correspond to triplicate experiments.

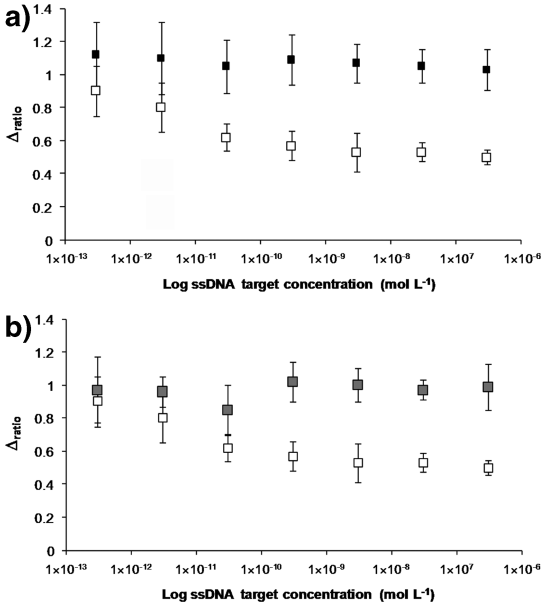

Figure 3. Impedimetric response toward the DNA target concentration in the case of hybridization with: (a) wild-type target (empty squares) and noncomplementary target (filled black squares); (b) wild-type target (empty squares) and mutant (filled gray squares). $\Delta_{ratio} = \Delta_s/\Delta_p$, $\Delta_s = R_{ct\ (sample)} - R_{ct\ (blank)}$; $\Delta_p = R_{ct\ (probe)} - R_{ct\ (blank)}$. Error bars correspond to triplicate experiments.

the negatively charged redox couple, thus increasing the R_{ct} value. Another factor that contributes to the R_{ct} increment is the steric hindrance introduced with the formation of the DNA probe film on the electrode surface. After hybridization with the wild-type target, a significant decrease in charge transfer resistance value was observed (red color). The R_{ct} decrease was less significant in the case of hybridization with mutant (green color), and no average R_{ct} variation was observed with the noncomplementary sequence (black color). As shown in the scheme, the reason for impedance decrease after hybridization with the complementary target can be due to the partial release of the hpDNA probes from the electrode surface. This should decrease the total charge present onto the electrode surface, thus reducing the resistance to charge transfer. When hybridization is less effective, as in the case of the mutant target, a lower amount of the hpDNA probes are expected to be released, thus resulting in a less significant R_{ct} decrease.

To obtain a reproducible sensing platform the hpDNA probe concentration to be immobilized onto the electrode surface was optimized at 1×10^{-5} M value for the three different graphene platforms (see Figure S2, Supporting Information). This concentration ensures full coverage of the electrode surface, avoiding any possible nonspecific adsorption of the DNA target. Even though a similar trend was obtained for the three different materials, a higher R_{ct} variation was shown for graphene-SL, indicating a larger amount of immobilized hpDNA probes. In Figure 2a the R_{ct} variation for the three different graphene platforms are represented at the optimized hpDNA concentration. As it can be observed in the figure, despite giving the highest signal, G-SL platform provided the worst reproducibility (RSD = 31%).

Figure 2b shows a comparison of results obtained for the impedimetric detection of DNA hybridization on the three different platforms. The signal represents R_{ct} variation due to hybridization with the wild-type relative to the negative control experiment (hybridization with a noncomplementary sequence). As shown in the histogram, the largest signal was obtained with the G-SL platform, together with the highest standard deviation (RSD = 20%). This result is consistent with previous data obtained for the optimization of hpDNA probes.

The impedimetric response toward the DNA target concentration was studied in order to be able to evaluate the limit of detection (LOD) for each of the three different platforms. For all platforms the impedimetric response after the hybridization step was recorded for ssDNA target concentrations from 3×10^{-12} to 3×10^{-7} M. The concentration of the hpDNA probe was kept constant at an optimized value of 1×10^{-5} M. In Figure 3a, the results obtained with the G-FL platform are represented as the relative R_{ct} variation between the values obtained in the different experiments (*i.e.*, DNA immobilization or hybridization) and the R_{ct} value due to the bare electrode (see $\Delta_{ratio} = \Delta_s/\Delta_p$; see the caption of Figure 3). As shown in the figure, increasing the target concentration led to a lower

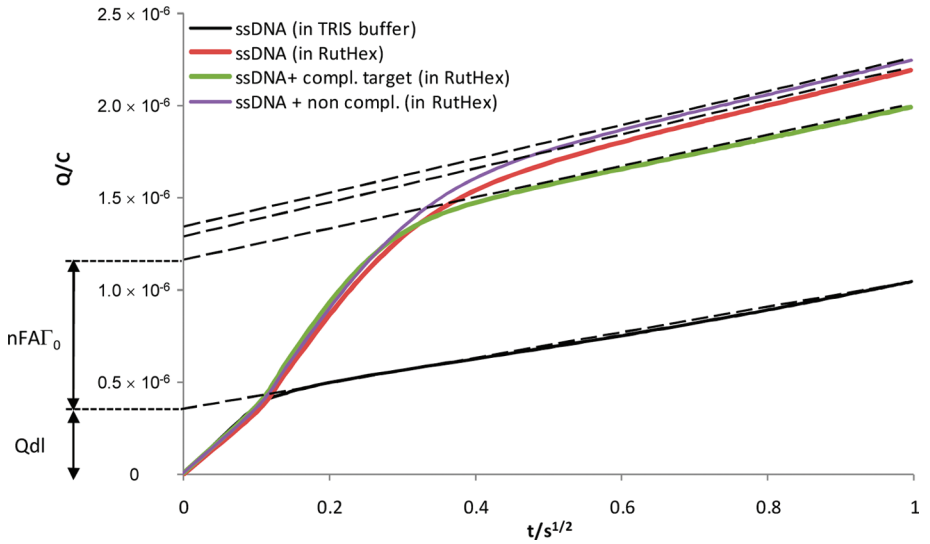

Figure 4. Chronocoulometry response curves for DNA modified electrodes.

analytical signal due to the decrease of R_{ct}, thus achieving a linear range between 3×10^{-13} and 3×10^{-10} M. After that, a plateau was reached and any further increase in the target concentration did not cause an additional change in the signal. When the noncomplementary sequence was employed in the hybridization step significant changes in R_{ct} were not recorded, thus confirming that nonspecific interactions can be considered negligible in this case. The same trend was observed for the each of the three different platforms employed, with the limit of detection for the wild-type target being 50 nM for graphene-SL, 6.6 pM for G-FL, and 66 μM for graphene-ML. These detection limits were calculated with consideration of the noise to be 3 times as high as the standard deviation of the value obtained in negative control experiments. The better LOD obtained with G-FL compared to G-SL is not surprising since the latter presented poor reproducibility for both hpDNA probe immobilization and detection of DNA hybridization, and these factors strongly influenced the detection limit. The low sensitivity obtained with G-ML is in agreement with the results obtained for hpDNA probe immobilization and hybridization detection on this platform.

Because of the results obtained, the most sensitive platform (G-FL) was chosen for the detection of SNP correlated to the development of Alzheimer's disease. As shown in Figure 3b the signal change recorded with the mutant sequence was lower than that obtained with the wild-type sequence, as expected. In fact hybridization with the mutant partially occurs, due to the presence of a SNP in the sequence. The differentiation between the wild type and mutant was detectable to 82 pM.

To better understand the hybridization mechanism, for the first time impedimetric results were compared to either chronocoulometry or fluorescence experiments on the same graphene platform. Chronocoulometry measurements showed that the total DNA density after hybridization with the complementary target was lower than that registered after DNA probe immobilization onto the electrode surface. This confirms that some hpDNA probes were released from the electrode surface during hybridization. The same experiment performed after hybridization with the noncomplementary target led to a slight increase in DNA density on the electrode surface, indicating that not only were the DNA probes not released but also that some nonspecific interactions occurred, leading to a partial nonspecific adsorption. In Figure 4 chronocoulometry response curves for DNA-modified electrodes are shown. By the use of the Cottrell[37] equation, the DNA density onto the electrode surface was calculated as the extrapolation of the intercept at time zero, and it was 1.98×10^{13} mol/cm^2 for hpDNA probes, 1.73×10^{13} mol/cm^2 for the wild-type (complementary target), and 2.04×10^{13} mol/cm^2 for non the complementary target.

For the fluorescence study we immobilized dye-tagged hpDNA probes onto the electrode surface.[21] When hybridization with the wild-type sequence occurred, we expected to observe some fluorescence signal in the remaining hybridization solution due to the release of the probes from the electrode surface. Obtained results confirmed our hypothesis, with the fluorescence obtained with the wild-type sequence being more significant than that measured with the noncomplementary target (for more details refer to Supporting Information).

To conclude we have developed a sensitive graphene platform for the detection of DNA hybridization and polymorphism using EIS as detection technique for the first time. Moreover we compared the performance of three different graphene platforms showing how different numbers of graphene sheets can affect

detection. We found that G-FL provided the best sensitivity and we employed this platform for the detection of SNPs. A higher sensitivity was obtained with impedimetric detection compared to that obtained with similar platform using fluorescence methods. We believe that the graphene-based strategy presented here could be used in the development of an analytical device for point-of-care diagnostic tests and for very sensitive detection of SNPs correlated to different diseases.

METHODS

G-SL, G-FL, and G-ML were immobilized onto each DEP chip surface by physical adsorption. Three μL of graphene at a concentration of 0.05 mg/mL in milli-Q water was deposited onto the electrode surface and allowed to dry at room temperature. Excess material that had not been absorbed was then removed from the electrode surface by gentle rinsing with milli-Q water. Before immobilization onto the electrode surfaces, the suspensions were sonicated for 10 min in order to achieve maximum dispersion of the material.

The probe oligonucleotide was immobilized onto the graphene surface by dry physical adsorption. A 3 μL volume of hpDNA probe in TSC1 buffer solution at the optimized concentration (see Supporting Information) was deposited onto the electrode surface for 10 min at 60 °C. The electrode was washed twice in TSC2 buffer with gentle stirring at room temperature to remove excess, nonadsorbed material. DEP chips modified with hpDNA probes were incubated in an Eppendorf tube with the hybridization solution (TSC1 buffer) containing the desired concentration of DNA target (total volume, 100 μL). The incubation was performed at 55 °C for 30 min, with gentle stirring. Two brief washing steps were then performed in TSC2 buffer at 42 °C.

For chronocoulometry experiments the DNA surface density before and after the hybridization step was determined using a method based on that reported by Steel *et al.*[38] The hexaammineruthenium(III) concentration used in the experiments was optimized at 25 μM (as determined by measuring the adsorption isotherm of the hpDNA modified electrode surface). Cottrell equation was used to calculate the DNA density onto the electrode surface as the extrapolation of the intercept at time zero.

For fluorescence experiments the same procedure was followed for the immobilization of FAM-hpDNA probes onto the electrode surface and hybridization with target. The fluorescence of the hybridization solution was analyzed by Carey Eclipse spectrofluorometer with excitation at 486 nm and emission range from 500 to 620 nm. Spectrometer slits were set for 5 nm band-pass.

Electrochemical experiments were performed with an Autolab potentiostat PGSTAT302 (Eco Chemie, Utrecht, The Netherlands) driven by GPES and FRA software version 4.9.

Impedance measurements were recorded between 0.1 MHz and 0.1 Hz at a sinusoidal voltage perturbation of 10 mV amplitude. The experiments were carried out at an applied potential of 0.15 V (*vs* a Ag/AgCl reference electrode) in a 0.1 M PBS buffer solution containing 10 mM $K_3[Fe(CN)_6]$/ $K_4[Fe(CN)_6]$ (1:1 molar ratio) as a redox probe. A Randles equivalent circuit was used to fit the obtained impedance spectra, represented as Nyquist plots in the complex plane. The χ^2 goodness of fit was calculated for each fitting by the Autolab Frequency Response Analyzer (FRA) software (Eco Chemie, The Netherlands).

Acknowledgment. The authors acknowledge NAP fund M58110000 (NTU, Singapore).

Supporting Information Available: Additional figures and discussion. This material is available free of charge *via* the Internet at http://pubs.acs.org.

REFERENCES AND NOTES

1. Zhai, J. H.; Cui, H.; Yang, R. F. DNA Based Biosensors. *Biotechnol. Adv.* **1997,** *15*, 43–58.
2. Murphy, L. Biosensors and Bioelectrochemistry. *Curr. Opin. Chem. Biol.* **2006,** *10*, 177–184.
3. Gorkin, R.; Park, J.; Siegrist, J.; Amasia, M.; Lee, B. S.; Park, J. M.; Kim, J.; Kim, H.; Madou, M.; Cho, Y. K. Centrifugal Microfluidics for Biomedical Applications. *Lab Chip* **2010,** *10*, 1758–1773.
4. Tsai, H. K. A.; Moschou, E. A.; Daunert, S.; Madou, M.; Kulinsky, L. Integrating Biosensors and Drug Delivery: A Step Closer toward Scalable Responsive Drug-Delivery Systems. *Adv. Mater.* **2009,** *21*, 656–661.
5. Xia, F.; Zuo, X. L.; Yang, R. Q.; Xiao, Y.; Kang, D.; Vallee-Belisle, A.; Gong, X.; Yuen, J. D.; Hsu, B. B. Y.; Heeger, A. J.; *et al.* Colorimetric Detection of DNA, Small Molecules, Proteins, and Ions Using Unmodified Gold Nanoparticles and Conjugated Polyelectrolytes. *Proc. Natl. Acad. Sci. U.S. A.* **2010,** *107*, 10837–10841.
6. Eggins, B. R. *Chemical Sensor and Biosensors*; Wiley: Northern Ireland (UK), 2002.
7. Madou, M. J. *Fundamentals of Microfabrication and Nanotechnology*; CRC Press: Boca Raton, FL, 2009.
8. Patolsky, F.; Lichtenstein, A.; Willner, I. Detection of Single-Base DNA Mutations by Enzyme-Amplified Electronic Transduction. *Nat. Biotechnol.* **2001,** *19*, 253–257.
9. Bonanni, A.; Esplandiu, M. J.; Valle, M. d. Impedimetric Genosensing of DNA Polymorphism Correlated to Cystic Fibrosis: A Comparison among Different Protocols and Electrode Surfaces. *Biosens. Bioelectron.* **2010,** *26*, 1245–1251.
10. Bonanni, A.; Pumera, M.; Miyahara, Y. Rapid, Sensitive, and Label-Free Impedimetric Detection of a Single-Nucleotide Polymorphism Correlated to Kidney Disease. *Anal. Chem.* **2010,** *82*, 3772–3779.
11. Star, A.; Tu, E.; Niemann, J.; Gabriel, J. C. P.; Joiner, C. S.; Valcke, C. Label-free Detection of DNA Hybridization Using Carbon Nanotube Network Field-Effect Transistors. *Proc. Natl. Acad. Sci. U.S.A.* **2006,** *103*, 921–926.
12. Kong, A.; Gudbjartsson, D. F.; Sainz, J.; Jonsdottir, G. M.; Gudjonsson, S. A.; Richardsson, B.; Sigurdardottir, S.; Barnard, J.; Hallbeck, B.; Masson, G.; *et al.*A High-Resolution Recombination Map of the Human Genome. *Nat. Genet.* **2002,** *31*, 241–247.
13. Wang, W. Y. S.; Barratt, B. J.; Clayton, D. G.; Todd, J. A. Genome-Wide Association Studies: Theoretical and Practical Concerns. *Nat. Rev. Genet.* **2005,** *6*, 109–118.
14. Rapley, R.; Harbron, S. *Molecular Analysis and Genome Discovery*; Wiley, New York, 2004.
15. Watson, J. D.; Baker, T. A.; Bell, S. P.; Gann, A.; Levine, M.; Losick, R. *Molecular Biology of the Gene*, 5th ed.; CSHL Press: 2004.
16. Lubin, A. A.; Plaxco, K. W. Folding-Based Electrochemical Biosensors: The Case for Responsive Nucleic Acid Architectures. *Acc. Chem. Res.* **2010,** *43*, 496–505.
17. Fan, C. H.; Plaxco, K. W.; Heeger, A. J. Electrochemical Interrogation of Conformational Changes as a Reagentless Method for the Sequence-Specific Detection of DNA. *Proc. Natl. Acad. Sci. U.S.A.* **2003,** *100*, 9134–9137.
18. Lin, Y. W.; Ho, H. T.; Huang, C. C.; Chang, H. T. Fluorescence Detection of Single Nucleotide Polymorphisms Using a Universal Molecular Beacon. *Nucleic Acids Res.* 2008, *36*.
19. Song, S. P.; Liang, Z. Q.; Zhang, J.; Wang, L. H.; Li, G. X.; Fan, C. H. Gold-Nanoparticle-Based Multicolor Nanobeacons for Sequence-Specific DNA Analysis. *Angew. Chem., Int. Ed.* **2009,** *48*, 8670–8674.

20. Miranda-Castro, R.; de-los-Santos-Alvarez, N.; Lobo-Castanon, M. J.; Miranda-Ordieres, A. J.; Tunon-Blanco, P. Structured Nucleic Acid Probes for Electrochemical Devices. *Electroanalysis* **2009,** *21*, 2077–2090.
21. Li, F.; Huang, Y.; Yang, Q.; Zhong, Z. T.; Li, D.; Wang, L. H.; Song, S. P.; Fan, C. H. A Graphene-Enhanced Molecular Beacon for Homogeneous DNA Detection. *Nanoscale* **2010,** *2*, 1021–1026.
22. He, S. J.; Song, B.; Li, D.; Zhu, C. F.; Qi, W. P.; Wen, Y. Q.; Wang, L. H.; Song, S. P.; Fang, H. P.; Fan, C. H. A Graphene Nanoprobe for Rapid, Sensitive, and Multicolor Fluorescent DNA Analysis. *Adv. Funct. Mater.* **2010,** *20*, 453–459.
23. Heller, A.; Feldman, B. Electrochemical Glucose Sensors and Their Applications in Diabetes Management. *Chem. Rev.* **2008,** *108*, 2482–2505.
24. Joo, S.; Brown, R. B. Chemical Sensors with Integrated Electronics. *Chem. Rev.* **2008,** *108*, 638–651.
25. Shao, Y. Y.; Wang, J.; Wu, H.; Liu, J.; Aksay, I. A.; Lin, Y. H. Graphene Based Electrochemical Sensors and Biosensors: A Review. *Electroanalysis* **2010,** *22*, 1027–1036.
26. Rao, C. N. R.; Sood, A. K.; Subrahmanyam, K. S.; Govindaraj, A. Graphene: The New Two-Dimensional Nanomaterial. *Angew. Chem., Int. Ed.* **2009,** *48*, 7752–7777.
27. Pumera, M. Graphene-Based Nanomaterials and Their Electrochemistry. *Chem. Soc. Rev.* **2010,** *39*, 4146–4157.
28. Davies, T. J.; Hyde, M. E.; Compton, R. G. Nanotrench Arrays Reveal Insight into Graphite Electrochemistry. *Angew. Chem., Int. Ed.* **2005,** *44*, 5121–5126.
29. Macdonald, J. R. *Impedance Spectroscopy*. Wiley: New York, 1987.
30. Gabrielli, C. *Use and Application of Electrochemical Impedance Techniques*. Solartron Analytical: Farnborough, UK, 1990.
31. Pejcic, B.; De Marco, R. Impedance Spectroscopy: Over 35 Years of Electrochemical Sensor Optimization. *Electrochim. Acta* **2006,** *51*, 6217–6229.
32. Willner, I.; Zayats, M. Electronic Aptamer-Based Sensors. *Angew. Chem., Int. Ed.* **2007,** *46*, 6408–6418.
33. Hardy, J.; Gwinn-Hardy, K. Genetic Classification of Primary Neurodegenerative Disease. *Science* **1998,** *282*, 1075–1079.
34. Roses, A. D. Apolipoprotein E Alleles as Risk Factors in Alzheimer's Disease. *Annu. Rev. Med.* **1996,** *47*, 387–400.
35. Das, H. K.; McPherson, J.; Bruns, G. A. P.; Karathanasis, S. K.; Breslow, J. L. Isolation, Characterization, and Mapping to Chromosome-19 of the Human Apolipoprotein-E Gene. *J. Biol. Chem.* **1985,** *260*, 6240–6247.
36. Rall, S. C.; Weisgraber, K. H.; Mahley, R. W. Human Apolipoprotein E—The Complete Aminoacid Sequence. *J. Biol. Chem.* **1982,** *257*, 4171–4178.
37. Keighley, S. D.; Li, P.; Estrela, P.; Migliorato, P. Optimization of DNA Immobilization on Gold Electrodes for Label-free Detection by Electrochemical Impedance Spectroscopy. *Biosens. Bioelectron.* **2008,** *23*, 1291–1297.
38. Steel, A. B.; Herne, T. M.; Tarlov, M. J. Electrochemical Quantitation of DNA Immobilized on Gold. *Anal. Chem.* **1998,** *70*, 4670–4677.